

lands, to be published).

³Bartsch et al., Ref. 1; Berlinghieri et al., Ref. 1. Evidence for the L in the mode $K^*(1400)\pi$ has also been presented by G. Bassompierre et al., Ref. 2.

⁴A. C. Callahan, S. Borenstein, D. Denegri, D. Ellis, L. Ettliger, D. Gillespie, G. Luste, E. Moses, A. Pevsner, and R. Zdanis, paper presented at the Third Topical Conference on Resonant Particles, Athens, Ohio, 1967 (unpublished).

⁵H. Foelsche et al., Rev. Sci. Instr. **38**, 879 (1967).

⁶We have used the Hulthén wave-function form factor with $\alpha = 45.5$ MeV and $\beta = 7\alpha$. M. Gourdin and A. Martin, Nuovo Cimento **11**, 670 (1959); S. Fernbach, R. A. Green, and K. M. Watson, Phys. Rev. **84**, 1084 (1951).

⁷As shown in Ref. 4, the low-mass $K^*\pi$ enhancement cannot be explained in terms of the deuteron form factor together with a reasonable $\exp(\lambda)$ dependence.

⁸See, for example, G. Bassompierre et al. (CERN-Bruxelles-Birmingham Collaboration), Phys. Letters **26B**, 30 (1967).

⁹We have used 840 to 940 MeV as the $K^*(890)$ and

1330 to 1540 as the $K^*(1400)$ mass regions.

¹⁰J. F. Allard et al. (Orsay-Ecole Polytechnique-Milan-Saclay-Berkeley Collaboration), Phys. Letters **19**, 431 (1965).

¹¹D. R. O. Morrison, Phys. Rev. **165**, 1699 (1968).

¹²M. Ross and Y. Y. Yam, Phys. Rev. Letters **19**, 546 (1967). See this paper for references to earlier work on the subject of diffraction dissociation or Deck effect.

¹³G. C. Fox and Elliot Leader, Phys. Rev. Letters **18**, 628 (1967). See also Ref. 11.

¹⁴All the following predicted distributions are obtained by assuming that the $K^-\pi^+\pi^-$ system is made by 0^+ exchange. They can be found, also, in C. Zemach, Phys. Rev. **133**, B1201 (1964).

¹⁵M. Jobs et al. (Birmingham-CERN-Bruxelles Collaboration), Phys. Letters **26B**, 49 (1967).

¹⁶The Yale group studying $K^-p \rightarrow L^-p$ at 12.6 BeV/c do not see evidence for a $K^-\omega$ decay mode of the L : J. Lach et al., Bull. Am. Phys. Soc. **13**, 114 (1968). This mode was previously one of the principal means for determining the isospin of the L : J. Bartsch et al., Ref. 1.

SPECTRUM OF NEUTRONS FROM MUON CAPTURE IN SILICON, SULFUR, AND CALCIUM*

R. M. Sundelin, R. M. Edelman, A. Suzuki,† and K. Takahashi‡

Carnegie-Mellon University, Saxonburg, Pennsylvania

(Received 27 March 1968)

The energy spectrum of neutrons emitted following the capture of negative muons in silicon, sulfur, and calcium has been measured between 7.7 and 52.5 MeV. The spectra were found to decrease exponentially with energy in the three cases, and no evidence was found for excitation of giant dipole resonances.

The neutron-energy spectrum can be represented as the sum of the evaporation spectrum,¹ the giant-resonance spectrum,² and the direct spectrum.^{3,4} A measurement of the total spectrum provides information concerning the contribution of each component, since the shapes of the three contributing spectra differ. In addition, the shape of each of these components depends on the nuclear model used, so that the validity of various models can be tested. The expected asymmetry of the neutrons is a function of the mechanism by which they are produced and of their energy; so a measurement of the energy spectrum of the neutrons is important for the interpretation of the measured asymmetry.

Experiment.—This experiment⁵ was performed using the negative beam from the muon channel of the Carnegie-Mellon University synchrocyclotron. The following paper discusses the data on neutron asymmetries, which were studied at the same time. Negative muons were stopped in the target, as shown in Fig. 1. Neutrons emitted fol-

lowing muon capture by a target nucleus were detected in counter 5.

The time between the stopping of a muon and the detection of an event in counter 5 was measured by a 100-MHz digital timing system. This time and the pulse height in counter 5 were simultaneously measured, and this two-dimensional information was stored in a 1600-channel pulse-height analyzer. The time measurement permits the accurate subtraction of background events. The neutron-energy spectrum was determined by unfolding the observed pulse-height spectrum.

Target stops were defined by 123469. Stops in counter 4 were rejected by a technique employing the pulse heights in counters 3 and 4.⁶

Counter 5 comprised a volume of NE-213 liquid scintillator viewed by a 58AVP photomultiplier. Pulse-shape discrimination was used to distinguish gammas from neutrons. A neutron event was defined by 569 in coincidence with a pulse-shape discriminator (PSD) pulse. A decay-

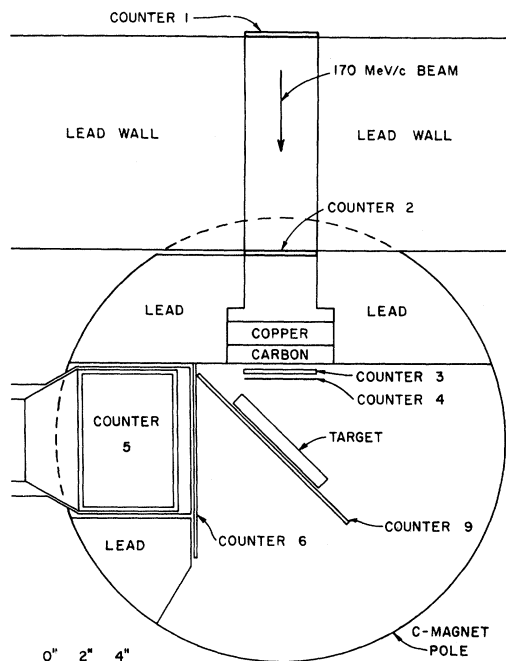


FIG. 1. Experimental apparatus.

electron event was defined by 569. The decay-electron-time spectrum was recorded at the same time as the neutron-time spectra, and provided normalization of the neutron spectrum.

The silicon, sulfur, and calcium targets each presented a thickness of 4 g/cm^2 to the beam. This thickness provided an adequate muon stopping rate, but did not appreciably scatter the neutrons and electrons emerging from the target. That the electron scattering was negligible was verified by also using targets of sulfur and calcium that were 2 and 1 g/cm^2 , respectively. All targets were chemically pure, and of natural isotopic composition.

The pulse-height response of counter 5 was measured by stopping negative pions in the target. Neutrons resulting from the pion capture were detected in counter 5, which was placed 1.5 m from the target for this measurement. The time of flight of the neutrons was measured using a time-to-pulse-height converter. Since the pions are captured in a time short compared with the neutron time of flight, the pion stopping signal served as a start signal for the time-of-flight measurement. The pulse-height response of the liquid scintillant is a nonlinear function of the recoil-proton energy, and the maximum pulse height observed for each neutron energy represented the pulse height due to a proton of nearly the same energy. The neutron time-of-

flight measurement also provided verification of the proper operation of the pulse-shape discriminator, since the time of flight unambiguously separated gammas and neutrons. The pulse-height spectra associated with each neutron energy provided verification of the Monte Carlo calculations which are discussed below.

Spectrum analysis and results.—The pulse-height spectra obtained from the pion-capture neutron time-of-flight measurements could not be used directly for obtaining the muon-capture neutron spectra from the observed pulse-height spectra for several reasons. Primarily, the number of neutrons produced in each energy interval following pion capture is not known precisely. In addition, the geometry differed in the two cases, causing a change in the effective solid angle and in the shapes of the spectra produced. In the time-of-flight measurement, the finite resolution of the timing system and the finite width of the timing window caused a widening of the resultant pulse-height spectra.

A Monte Carlo calculation was performed to simulate the pion-capture neutron time-of-flight measurement. The measurement was used to verify the calculation below 17.5 MeV . Above 17.5 MeV , the $C(n, p)B$ cross section, which has not been measured over the entire region of interest, is significant, and this cross section was determined by comparing the Monte Carlo results with the measured spectra.

Another Monte Carlo calculation was performed to determine the stopping distribution of the muons in the target and to simulate the muon-capture neutron measurement for a number of different neutron energies.

The results of the Monte Carlo calculations for the muon-capture neutrons were used to unfold the neutron spectra from the measured pulse-height spectra. Energy histograms are plotted in Fig. 2, and integral and differential spectra are presented in Table I.

The neutron-energy spectra for the three elements studied are quite similar. It is noted that, within the errors, all of the neutron spectra can be fitted with decaying exponentials. The characteristic decay constants of the observed exponentials are 7.6 , 7.3 , and 7.2 MeV for silicon, sulfur, and calcium, respectively.

The shape of the spectrum for calcium agrees in the region of overlap, from 7.7 to 16 MeV , with the unnormalized spectrum measured by Haggé.⁷ The calcium spectrum also agrees, in the region of overlap from 7.7 to 50 MeV , with

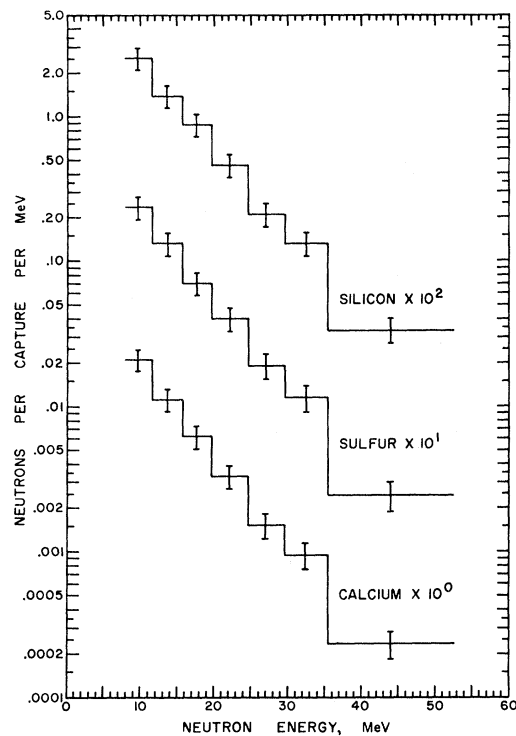


FIG. 2. Energy histograms.

the normalized spectrum measured by Turner.⁸

The spectra do not exhibit the peaks predicted by the giant-resonance calculations,⁹ although it is possible that all giant-resonance peaks with significant amplitudes lie below the lowest threshold in this experiment.¹⁰ The measured spectra exceed the direct spectra predicted using a modified Fermi-gas model in both magnitude and maximum energy,¹¹ and, above 7.7 MeV, exceed the direct-spectrum magnitudes predicted using the shell model by factors of the order of 30.¹² The origin of these high-energy neutrons is not presently understood.

*Work supported by the U. S. Atomic Energy Commission.

†Present address: Physics Department, University of Chicago, Chicago, Ill.

‡Present address: Physics Department, Tohoku University, Sendai, Japan.

¹V. Weisskopf, Phys. Rev. **52**, 295 (1937).

²J. Tiomno and J. A. Wheeler, Rev. Mod. Phys. **21**, 144 (1949); J. R. Luyten, H. P. C. Rood, and H. A. Tol-

Table I. Differential and integral spectra. E_{\min} and E_{\max} are the energy interval limits in MeV.

Target	E_{\min} MeV	E_{\max} MeV	Neutrons per Capture per MeV	Neutrons per Capture Above E_{\min}		
Si	7.73	11.49	0.0251	± 0.0044	0.232	± 0.041
	11.49	15.62	0.0138	± 0.0024	0.138	± 0.025
	15.62	19.54	0.0087	± 0.0015	0.081	± 0.015
	19.54	24.55	0.00461	± 0.00082	0.0469	± 0.0086
	24.55	29.41	0.00210	± 0.00039	0.0238	± 0.0045
	29.41	35.34	0.00132	± 0.00025	0.0136	± 0.0026
S	7.73	11.49	0.0234	± 0.0041	0.210	± 0.037
	11.49	15.62	0.0132	± 0.0023	0.122	± 0.022
	15.62	19.54	0.0070	± 0.0012	0.068	± 0.013
	19.54	24.55	0.00401	± 0.00072	0.0403	± 0.0077
	24.55	29.41	0.00191	± 0.00037	0.0202	± 0.0041
	29.41	35.34	0.00114	± 0.00023	0.0109	± 0.0023
Ca	7.73	11.49	0.0210	± 0.0036	0.183	± 0.032
	11.49	15.62	0.0111	± 0.0019	0.104	± 0.019
	15.62	19.54	0.0062	± 0.0011	0.058	± 0.011
	19.54	24.55	0.00330	± 0.00059	0.0335	± 0.0063
	24.55	29.41	0.00152	± 0.00029	0.0170	± 0.0034
	29.41	35.34	0.00094	± 0.00019	0.0096	± 0.0020
	35.34	52.53	0.00023	± 0.00005	0.0040	± 0.0008

hoek, Nucl. Phys. **41**, 236 (1963); L. L. Foldy and J. D. Walecka, Nuovo Cimento **34**, 1026 (1964).

³E. Lubkin, Ann. Phys. (N.Y.) **11**, 414 (1960).

⁴E. Dolinskii and L. Blokhintsev, Zh. Eksperim. i Teor. Fiz. **35**, 1488 (1958) [translation: Soviet Phys.-JETP **8**, 1040 (1959)]; M. Akimova, L. Blokhintsev, and E. Dolinskii, Zh. Eksperim. i Teor. Fiz. **39**, 1806 (1960) [translation: Soviet Phys.-JETP **12**, 1260 (1961)].

⁵R. M. Sundelin, Carnegie Institute of Technology Report No. CAR-882-22, 1967 (unpublished).

⁶R. M. Sundelin and K. Takahashi, Nucl. Instr. Methods **54**, 250 (1967).

⁷D. Hagge, University of California Report No. UCRL-10516, 1963 (unpublished).

⁸L. Turner, Carnegie Institute of Technology Report No. CAR-882-5, 1964 (unpublished).

⁹H. Überall, Phys. Rev. **139**, B1239 (1965).

¹⁰L. L. Foldy and R. H. Klein, Case Institute of Technology and Western Reserve University Report No. COO-1573-14, 1967 (unpublished).

¹¹See Ref. 3.

¹²See Ref. 4.